

Global coronal waves

Chen P. F.

School of Astronomy and Space Science, Nanjing University, 163 Xianlin Avenue, Nanjing 210023, China
chenpf@nju.edu.cn

Abstract. After the *Solar and Heliospheric Observatory (SOHO)* was launched in 1996, the aboard Extreme Ultraviolet Imaging Telescope (EIT) observed a global coronal wave phenomenon, which was initially named “EIT wave” after the telescope. The bright fronts are immediately followed by expanding dimmings. It has been shown that the brightenings and dimmings are mainly due to plasma density increase and depletion, respectively. Such a spectacular phenomenon sparked long-lasting interest and debates. The debates were concentrated on two topics, one is about the driving source, and the other is about the nature of this wavelike phenomenon. The controversies are most probably because there may exist two types of large-scale coronal waves that were not well resolved before the *Solar Dynamics Observatory (SDO)* was launched: one is a piston-driven shock wave straddling over the erupting coronal mass ejection (CME), and the other is an apparently propagating front, which may correspond to the CME frontal loop. Such a two-wave paradigm was proposed more than 13 years ago, and now is being recognized by more and more colleagues. In this paper, we review how various controversies can be resolved in the two-wave framework and how important it is to have two different names for the two types of coronal waves.

1. Introduction

After the launch of the *Solar and Heliospheric Observatory (SOHO)* in December 1995, the onboard Extreme Ultraviolet (EUV) Imaging Telescope [EIT, *Delaboudinière et al.*, 1995] was routinely observing the solar corona with a cadence of 12–15 min at four EUV wavelengths, Fe IX 171 Å, Fe XII 195 Å, Fe XV 284 Å, and He II 304 Å. On 1997 May 12, the EIT telescope observed an intermediate-scale solar flare in the northern hemisphere. The flare was registered as C1.3-class according to its peak flux at 1–8 Å measured by the *Geostationary Operational Environmental Satellites (GOES)*. Looking at the original images, one can only identify a small-sized brightening of the flare and some perturbation in the background, with nothing special. However, after using a running difference technique, i.e., to subtract each image with one measured at the previous time so as to enhance any weak variations, *Thompson et al.* [1998] discovered an unexpected yet spectacular phenomenon in the corona. It is seen that a wavelike pattern propagated outward across the major part of the solar disk, starting from the source active region of the solar flare, as displayed by Figure 1. The propagating wave front is immediately followed by an expanding dimming. The brightening of the fronts is visible at EUV spectral lines with different formation temperatures, implying that they are mainly due to density enhancement [*Wills-Davey and Thompson*, 1999]. The amplitude of the brightening along the fronts is averaged to be below 25% [*Thompson et al.*, 1999]. Since the wavelike phenomenon was discovered with the EIT telescope, it was then called “EIT wave”. Arguing that it might not be appropriate to name a phenomenon after an instrument, colleagues invented several new terms for it [see *Chen and Fang*, 2012, for details], such as “EUV wave” [*Webb*, 2000], “global coronal wave” [*Hudson*, 1999], “large-scale coronal waves” [*Sterling and Hudson*, 1997], “coronal propagating front” [*Schrijver et al.*, 2011], “large-scale coronal

propagating front” [*Nitta et al.*, 2013]. In this paper, we tend to use “EUV waves” for any kind of wavelike phenomena observed in EUV and “EIT waves” for the phenomenon discovered by [*Thompson et al.*, 1998]. The coronal EUV waves are different from those waves which are trapped inside magnetic loops of an active region [*Aschwanden et al.*, 1999; *Nakariakov et al.*, 1999; *Wang*, 2015], confined along large-scale interconnecting loops [*Liu et al.*, 2012], or in the coronal holes [*Banerjee and Krishna Prasad*, 2015].

For an elastic medium like the solar corona, any local perturbation, e.g., in thermal pressure, magnetic field, or velocity, would result in resistance from the medium. Such resistance is always accompanied by a restoring force, by which the perturbed part starts to oscillate locally. The oscillation will perturb the neighboring parts of the medium. Like a chain reaction, a perturbation would propagate out as a wave phenomenon, which manifests itself as a propagating pattern. However, when a propagating pattern is observed, we sometimes fall into the trap of black-or-white thinking. When we are sure that the observed moving feature is not mass motion (e.g., when the Doppler velocity is much smaller than the propagation velocity even after correcting of the projection effects), we might claim that it is a wave. In this case we forget the third possibility, i.e., it could be an apparent motion. For example, the successive brightening of auroras is a kind of apparent motion, neither a mass motion nor a wave. The discovery and the ensuing interpretation of the globally propagating waves in the solar corona, i.e., “EIT waves”, are an excellent example to illustrate how complicated a propagating pattern would be. This paper is intended to review the progress on this global coronal wave in the past 18 years. In order not to confuse the readers, we try to describe the contents in a self-consistent way, which is inevitably influenced by the author’s own opinion. For more balanced descriptions among different theoretical models, the readers are referred to the reviews by *Wills-Davey and Attrill* [2009], *Warmuth* [2010], *Gallagher and Long* [2011], *Zhukov* [2011], *Chen and Fang* [2012], *Patsourakos and Vourlidas* [2012], and *Liu and Ofman* [2014].

2. Chromospheric Moreton Waves

It is nearly impossible to talk about “EIT waves” without mentioning chromospheric Moreton waves.

In 1960s, with the aim to detect Doppler-shifted features, *Moreton and Ramsey* [1960] used H α -0.5 Å waveband to observe solar flares. As a by product, they found a bright front in the H α -0.5 Å images propagating outward to a distance of $\sim 10^5$ km with a velocity of 500–2000 km s $^{-1}$. This phenomenon was later widely called “Moreton waves”. The wave fronts are bright in H α center and the blue wing, while dark in the H α red wing.

These observational features, i.e., the high speed, the long distance, and the weak amplitude, posed a serious challenge for a straightforward interpretation, as shown as follows. The solar atmosphere is composed of a thin photosphere at the solar surface with a thickness of ~ 500 km, a slightly thicker chromosphere above the photosphere (~ 2000 km), and a vast corona extending outward to the whole heliosphere. The plasma density drops drastically from the photosphere to the chromosphere, and further to the corona. However, the magnetic field decreases with height more gently. As a result, the Alfvén velocity $v_A = B/\sqrt{\mu_0\rho}$ increases rapidly from ~ 10 km s $^{-1}$ in the photosphere to ~ 100 km s $^{-1}$ in the chromosphere, and further up to ~ 1000 km s $^{-1}$ in the corona. The H α spectral line, with which Moreton waves are observed, is formed in the chromosphere. It means that Moreton waves are a phenomenon happening in the chromosphere. Because the Alfvén velocity in the chromosphere is of the order of ~ 100 km s $^{-1}$, if Moreton waves, which are observed in the chromosphere with a propagation velocity of 500–2000 km s $^{-1}$, are real waves propagating in the chromosphere, their Alfvénic Mach number should be around 5–20, i.e., they must be very strong shock waves. However, without continual piston-driving, such strong shock waves would decay rapidly as they propagate outward so that they cannot reach a distance of the order of 10^5 km as found by *Moreton and Ramsey* [1960]. Therefore, the high velocity and the long propagation distance of the chromospheric Moreton waves are conflicting characteristics apparently. Besides, if Moreton waves are such strong shock waves, the amplitude of the wave should be huge. However, Moreton wave fronts are very faint, and the associated Doppler velocity is only about 6–10 km s $^{-1}$ [*Svestka*, 1976]. These features puzzled solar physicists for quite a long time.

Several possibilities were put forward, but the basic idea was the same: Moreton waves are related to waves propagating in the corona [*Carmichael*, 1964; *Meyer*, 1968]. A proper treatment was conducted by *Uchida* [1968], who proposed that the pressure pulse in the solar flare generates a fast-mode magnetohydrodynamic (MHD) wave propagating in the corona. The skirt of the wave front sweeps the chromosphere, pushing the chromospheric material downward, by which a Moreton wave front is formed. Such a process is illustrated in Figure 2. The basic framework of Uchida’s model is correct, the main modification we made in Figure 2 is that the coronal counterpart of a Moreton wave is driven by the eruption of a flux rope with a filament at the bottom (note that the filament is often identified as the core of a CME), i.e., the coronal counterpart of any Moreton wave is a piston-driven shock wave straddling over the ejecta, rather than a blast wave initiated by the pressure pulse in the accompanied solar flare [see also *Cliver et al.*, 1999; *Chen et al.*, 2002].

According to the modified Uchida model in Figure 2, the erupting flux rope drives a fast-mode coronal shock wave (*red lines*) propagating outward. During the time interval from t_1 to t_2 , the footpoint of the coronal shock wave moves from point A to point B with a velocity of ~ 1000 km s $^{-1}$. At the same time, the wave front in the chromosphere also propagates from CA to DB with a velocity of ~ 100 km s $^{-1}$.

Since the fast-mode wave velocity in the chromosphere is ~ 10 times smaller than that of the coronal fast-mode wave, the propagation distance between the two fronts DB and CA would be ~ 10 times shorter than that of the two coronal fronts at the time t_2 and t_1 . As a result, the real wave fronts in the chromosphere would be strongly oblique as shown by the blue lines in Figure 2. The forward-inclined wave front was inferred by observations [*Vršnak et al.*, 2002; *Gilbert et al.*, 2008]. According to the radiative transfer calculations, the emissions of the H α line profile at different wavelengths come from different layers of the chromosphere, say, the H α line center is formed in the upper chromosphere, whereas the H α line wings are formed in the lower chromosphere [*Vernazza et al.*, 1981]. In observations, Moreton waves are generally detected with H α filtergrams using a narrow waveband in the H α profile, e.g., H α -0.5 Å [*Moreton and Ramsey*, 1960]. The emission is mainly from a certain layer of the chromosphere. Without loss of generality, we can assume the chosen H α waveband is formed at the level G, which intersects with the two chromospheric fronts at points E and F as indicated by the dashed line in Figure 2. As a result, an H α Moreton wave front would be seen to propagate from point E to point F, which is equivalent to the distance from point A to point B, i.e., the H α Moreton wave has the same velocity as the footprint of the coronal fast-mode wave, though lagging behind. Such a spatial delay of about tens of Mm was clearly found in observations by *Vršnak et al.* [2002] and recently by *White et al.* [2013], and was reproduced by simulations as well [*Chen et al.*, 2005a]. The co-spatiality between the H α Moreton wave and the coronal shock wave mentioned in some observations [e.g., *Asai et al.*, 2012; *Shen and Liu*, 2012] is just an approximation due to limited spatial resolution. It is also seen that the wave fronts in the chromosphere are nearly horizontal due to the significant difference between the fast-mode MHD wave speeds in the corona and in the chromosphere. Hence it is expected that the Doppler velocity of the chromospheric plasma in the downstream of the fast-mode MHD wave, which is mainly perpendicular to the wave front, is downward. The downward motion results in a red shift of the H α line profile, producing brightening in the blue wing of the H α line and darkening in the red wing. The intensity at H α line center is also slightly increased. It was shown that the intensity variation due to the red shift of the chromosphere peaks at H $\alpha \pm 0.45$ Å [*Chen et al.*, 2005a], meaning that H $\alpha \pm 0.45$ Å might be the best passband for the detection of Moreton waves using filtergrams. The essence of Uchida’s model is that the chromospheric Moreton wave itself is not a wave, it is the footprint of the fast-mode coronal wave. Since the fast-mode wave speed in the corona is of the order of 1000 km s $^{-1}$, when an H α Moreton wave is observed to travel with a speed higher than 1000 km s $^{-1}$, the coronal counterpart of the Moreton wave is either a simple wave or a weak shock wave. This then explains why it can propagate for a long distance and the amplitude of the wave front is small.

Based on Uchida’s model, a fast-mode coronal Moreton wave is expected to exist, which was called coronal Moreton wave by *Krucker et al.* [1999], *Torsti et al.* [1999], and *Thompson et al.* [1999].

3. Are “EIT waves” the expected coronal Moreton waves?

When coronal “EIT waves” were discovered [*Moses et al.*, 1997; *Thompson et al.*, 1998], they were thought to be the long-awaited coronal Moreton waves, i.e., fast-mode MHD waves or shock waves [*Thompson et al.*, 1999; *Wang*, 2000; *Wu et al.*, 2001; *Ofman and Thompson*, 2002; *Selwa et al.*, 2013]. There are several reasons for the deduction. First,

any coronal mass ejection (CME)/flare eruption should excite fast-mode MHD waves, and only “EIT waves” were observed, therefore, “EIT waves” *should* be fast-mode MHD waves. Second, at one moment in two events, the “EIT wave” front was found to be nearly cospatial with the H α Moreton wave front [Thompson *et al.*, 2000; Pohjolainen *et al.*, 2001]. However, the observed “EIT waves” showed more features that cannot be accounted for in terms of fast-mode MHD waves.

If “EIT waves” were the fast-mode coronal Moreton waves, there should be strong correlation between the “EIT wave” speed and the speed of type II radio bursts since the latter result from the same shock wave as the Moreton wave [Uchida, 1974]. However, Klassen *et al.* [2000] found that there is a lack of correlation between the “EIT wave” speed and the speed of type II radio bursts. Furthermore, Klassen *et al.* [2000] and Zhang *et al.* [2011] revealed that the “EIT wave” speed is typically three times smaller than the Moreton wave speed (or the propagation speed of the type II radio burst). More seriously, “EIT wave” speed can be well below the sound speed in the corona [Tripathi and Raouafi, 2007; Thompson and Myers, 2009], sometimes even down to $\sim 10 \text{ km s}^{-1}$ [Zhukov *et al.*, 2009].

If “EIT waves” were the fast-mode coronal Moreton waves, it is then expected to see a strong positive correlation between the “EIT wave” speed and the local magnetic field strength if the plasma density does not change much. However, Yang and Chen [2010] found that the “EIT wave” speed is negatively correlated with the magnetic field strength. It is noticed that Zhao *et al.* [2011] obtained the opposite conclusion by checking the correlation between the “EIT wave” speed and the local fast-mode wave speed (v_f). On the one hand, it is more appropriate to compare the “EIT wave” speed with v_f as in Zhao *et al.* [2011] rather than just the magnetic field strength as done by Yang and Chen [2010]. On the other hand, the “EIT wave” event analyzed by Zhao *et al.* [2011] was on the east limb, and the photospheric magnetogram used in their modeling was actually measured about one week later, hence it might not represent the real situation when the “EIT wave” was propagating. Besides, the assumed coronal density in Zhao *et al.* [2011] is so high and the resulting Alfvén speed is so low, e.g., even $< 100 \text{ km s}^{-1}$, that the “EIT wave” in their model would be a strong shock wave, which might not be able to explain the small amplitude of the “EIT wave” fronts.

If “EIT waves” were the fast-mode coronal Moreton waves, they would be concentrated toward regions of smaller fast-mode speeds (probably weaker magnetic fields, assuming that the plasma density does not vary much) due to refraction, showing no systematic pattern related to the helicity of the source active region. However, with 8 examples Attrill *et al.* [2007; 2014] revealed that the rotation of “EIT wave” fronts, a feature discovered by Podladchikova and Berghmans [2005], shows a systematic helicity rule, i.e., being anticlockwise when the source active region has negative helicity and clockwise when the source active region has positive helicity. The sense of rotation is the same as the erupting filaments, which are untwisting during eruptions [Chen, 2011].

There are many other features of “EIT waves” that cannot be explained simply by the fast-mode wave model. For example, Chen *et al.* [2011] found that the plasma outflow in a small coronal hole diminished after an “EIT wave” passed by. Chen [2009a] and Dai *et al.* [2010] claimed that the “EIT wave” front is cospatial with the CME frontal loop. Well before these work, it is Delannée and Aulanier [1999] and Delannée [2000] who first challenged the fast-mode wave model for “EIT waves”. In three events, they found that a stationary wave front was located at a magnetic separatrix, across which the magnetic field strength might change smoothly but the magnetic fields on its two sides belong to

different magnetic systems. This feature is difficult to be accounted for by the fast-mode wave model. They explained it to be due to the opening of the closed magnetic field lines. It is noted in passing here that the stationary EUV front mentioned above might not be concluding evidence against the fast-mode MHD wave. For example, Kwon *et al.* [2013] found that two stationary EUV fronts located on the two footpoints of a streamer brightened soon after a fast-mode MHD wave swept the upper streamer. They explained the stationary EUV fronts as trapped fast-mode waves due to the deflection of the streamer. On the other hand, it is commented by B. Vršnak (2015, private communication) that these two fronts are actually moving away from each other slightly, rather than being stationary, and the two separating fronts might be similar to flare ribbons due to magnetic reconnection of the current sheet above the streamer, which was triggered by the transiting fast-mode wave.

4. Toward a better model

Inspired by the questioning by Delannée [2000], Chen *et al.* [2002] performed MHD numerical simulations to examine what wave phenomena would appear during CME eruptions. In their MHD numerical results, as a flux rope erupts, two types of wavelike phenomena appear in the corona. The faster one is a piston-driven shock wave straddling over the erupting flux rope. The leg of this wave travels outward at a speed 773 km s^{-1} in the horizontal direction, and was proposed to be the coronal Moreton wave. The slower one also straddles over the erupting flux rope, but behind the coronal Moreton wave. The horizontal speed of its wave front is only 250 km s^{-1} . Chen *et al.* [2002] proposed that the slower wave corresponds to the “EIT wave” observed by Thompson *et al.* [1998], which is about 3 times slower than the coronal Moreton wave, consistent with observations [Klassen *et al.*, 2000; Zhang *et al.*, 2011]. In order to explain the unexpected “EIT wave”, Chen *et al.* [2002] noticed that as a flux rope erupts, all the closed magnetic field lines straddling over the flux rope would finally be stretched out, successively from the inner field lines to the outer field lines. For any individual field line, the stretching starts from the top, and is then transferred down to the footpoint of the field line. Based on this intuition, Chen *et al.* [2002] proposed the magnetic field-line stretching model for “EIT waves”, which is illustrated by Figure 3. Note that density enhancement is formed outside the field line when any part of the field lines is newly stretched, so all the stretching patches at one moment form a pattern, which is a domelike structure straddling over the erupting flux rope [Chen, 2009a], as found from observations [Veronig *et al.*, 2010].

According to this idea as illustrated in Figure 3, the corresponding apparent velocity of the “EIT wave” is $v_{\text{EIT}} = CD/\Delta t$, where the time difference between the successive formation of the “EIT wave” fronts at points D and C is expressed as $\Delta t = AB/v_f + (BD - AC)/v_A$, where $v_f = \sqrt{v_A^2 + c_s^2}$ and v_A are the fast-mode wave speeds across and along the field lines, respectively, v_A is the Alfvén speed, and c_s is the sound speed. For any prescribed magnetic distribution, we can always quantitatively derive the corresponding “EIT wave” velocity. For simplicity, Chen *et al.* [2002] assumed an ideal case where all the magnetic field lines overlying the flux rope are concentric semi-circles, and the corresponding “EIT wave” velocity is found to be $v_{\text{EIT}} = 0.34v_f$, i.e., the “EIT wave” speed is roughly 3 times smaller than the local fast-mode wave speed. This is consistent with the observations [Klassen *et al.*, 2000; Zhang *et al.*, 2011], as well as the MHD numerical simulations presented in Chen *et al.* [2002]. The large Doppler velocity and spectral line width immediately behind the “EIT wave” in the numerical simulations are consistent with those observed by Chen

et al. [2010]. Later, *Chen et al.* [2005b] illustrated how the magnetic fieldline stretching model can explain why “EIT waves” stop near magnetic separatrices and why there is no correlation between the “EIT wave” velocity and the speed of the type II radio bursts. One important prediction of the magnetic fieldline stretching model is that, given a sufficiently high time cadence, any EUV imaging telescope can observe two wavelike patterns, one is faster and the other is slower. It should be noted that the 3-fold relation between the faster wave and the slower wave is valid when the magnetic field lines overlying the flux rope are concentric semi-circles. If the magnetic field lines are elongated in the upward direction, the velocity ratio between the two waves is not necessarily to be 3. Therefore, the velocity ratio of 4 between two EUV waves found by *Zheng et al.* [2012a] does not conflict with the magnetic fieldline stretching model. It should be pointed out that in Figure 3 we assume for simplicity that the stretching is transferred from point A to C for the first EIT wave front, and then from point A to D via B for the next EIT wave front. In reality, the transfer of the stretching from point A to D may detour around point B, which would result in the widening of the EIT wave front during propagation as demonstrated by *Chen and Shibata* [2002]. Furthermore, it was proposed that a CME may experience a short period of overexpansion in the low corona [*Patsourakos et al.*, 2010]. In such a spherical piston-driven case, the stretching is transferred directly in the horizontal direction, and the EIT wave velocity would be identical to the fast-mode wave speed. This may explain why the slow “EIT wave” and the fast-mode wave are coupled in the early stage [*Cheng et al.*, 2012].

Since then, many other models have been proposed to explain the slow “EIT waves”. For example, *Attrill et al.* [2007] suggested that EIT wave fronts are produced when the erupting magnetic field lines reconnect with a series of low-lying antiparallel magnetic loops, as depicted by Figure 4 in their paper. Our opinions on this model are: (1) “EIT waves” are not a low-lying phenomenon. They often extend ~ 90 Mm above the solar surface [*Patsourakos et al.*, 2009], and sometimes are observed to have a domelike structure [*Veronig et al.*, 2010]. This issue has not yet been addressed in the successive reconnection model. (2) Whereas it is hard to see that all low-lying magnetic loops are antiparallel with the erupting field lines, there are occasionally antiparallel magnetic loops in the background, in which case magnetic reconnection between the erupting magnetic field and the background magnetic field can happen, as demonstrated by *Cohen et al.* [2009]. Therefore, the combination of this successive magnetic reconnection model and the magnetic fieldline stretching model can account for many observational features of “EIT waves”. *Delannée et al.* [2008] proposed a current shell model for “EIT waves”. In this model, “EIT waves” correspond to the current shell between the erupting core magnetic field and the potential background magnetic field. One feature of this model is that the footpoints of the current shell are fixed, therefore, the authors associate the propagating “EIT wave” fronts with the current shell at a certain height. *Downs et al.* [2012] reproduced such a current shell structure, which is confined to the region of CME itself and mismatches the outer EUV wave front. Our intuition is that the current-shell model might be applied to explain some looplike structures near the source active region during CMEs. *Wills-Davey et al.* [2007] proposed an idea related to slow-mode soliton waves, with the aim to explain the coherence of the propagating “EIT wave” fronts. One difficulty is that “EIT waves” propagate across magnetic field lines, whereas slow-mode waves propagate along magnetic field lines. Based on MHD numerical simulations, *Wang et al.* [2009] proposed that “EIT waves” might be due to the joint impact of the slow-mode shock waves and the vortices behind the erupting flux rope.

5. Evidence of two types of EUV waves

It is widely accepted that a full-fledged CME is composed of three components, i.e., a convex-outward frontal loop, an embedded bright core representing the erupting filament, and a cavity in between [*Forbes*, 2000]. Besides, a piston-driven shock, which is a fast-mode shock wave, frequently straddles over the frontal loop, producing type II radio bursts [*Wild et al.*, 1963] and manifesting itself in white-light coronagraph images [*Vourlidas et al.*, 2003]. All these observational results have led to a paradigm for CMEs as depicted by Figure 4, though one or two parts in the schematic sketch might not be present in an individual event. Now suppose such a complex structure as depicted in Figure 4 is observed from above by EUV telescopes, what wavelike patterns can be seen? We would expect to see both the piston-driven shock wave and the CME frontal loop propagating outward [*Patsourakos and Vourlidas*, 2012]. That is to say, even with an imaginary test, we would expect to see two wavelike phenomena in the EUV images of the solar disk based on the widely accepted CME model, with the first wave being faster than the second one.

From the observational point of view, the evidence of two EUV waves already existed in the *SOHO*/EIT observations, despite the low cadence of the telescope [*Warmuth and Mann*, 2011]. For example, *Biesecker et al.* [2002] found a special subclass of “EIT waves”, whose fronts are very sharp, in contrary to the diffuse fronts of ordinary “EIT waves”. This subclass of “EIT waves” should be the coronal Moreton waves, and indeed, in two events, these sharp “EIT waves” were found to be nearly cospatial with $H\alpha$ Moreton waves at a single moment [*Thompson et al.*, 2000; *Pohjola-lainen et al.*, 2001]. Note here again that the cospatiality occurs at only one moment, since $H\alpha$ Moreton waves are usually visible for < 10 min [*Francile et al.*, 2013], whereas the time cadence of the EIT telescope is 12–15 min. Unfortunately, the occasional cospatiality between the sharp “EIT wave” front and the $H\alpha$ Moreton wave can be easily considered to be the strong evidence to support the fast-mode wave model for “EIT waves”. To explain the velocity discrepancy between Moreton waves and “EIT waves” in the fast-mode wave model, it was then argued that the fast-mode wave decelerates later in the quiet Sun region [*Wu et al.*, 2001]. However, both the $H\alpha$ [*Eto et al.*, 2002] and radio [*White and Thompson*, 2005] observations did not show any significant deceleration of the Moreton wave.

The first observational evidence of two EUV waves was discovered by *Harra and Sterling* [2003], who used the high-cadence (1–2 min) data from the *Transition Region and Coronal Explorer (TRACE)* satellite. They found a brighter wave front moving with a velocity of ~ 200 km s $^{-1}$ and a weaker wave front moving with a velocity of ~ 500 km s $^{-1}$. It is a pity that the authors did not use a time-distance plot to clearly display the separation of the two waves so that their statement was questioned later. For example, *Wills-Davey* [2006] analyzed the same event and argued that only one wave exists. She considered the faster weak front ahead as a Gaussian extension of the slower bright front behind. However, in terms of a simple wave with certain extension as mentioned by *Wills-Davey* [2006], the wave portions with larger amplitudes should travel faster than those with smaller amplitudes. In this sense, the brighter and fainter fronts recognized by both *Harra and Sterling* [2003] and *Wills-Davey* [2006] are more likely to be two separate fronts.

After the *Solar Terrestrial Relations Observatory (STEREO)* twin satellites were launched in 2006, its on-board Extreme Ultra-Violet Imager (EUVI) with a higher

cadence (2.5 min) did not bring any breakthrough in resolving the theoretically predicted two types of EUV waves. Instead, most papers based on *STEREO*/EUVI data tend to support the fast-mode wave model for “EIT waves” [Long *et al.*, 2008; Gopalswamy *et al.*, 2009]. For example, Pat-sourakos and Vourlidas [2009] analyzed the first quadrature observations of an EIT wave event, and concluded that EIT waves are fast-mode waves. The reason is that they found that the EIT wave front is outside the CME bubble. We tend to think that their EIT wave front is cospatial with the CME bubble, which is especially clear at 05:55 UT in their Figure 1. The difficulty in matching an EIT wave with the CME bubble lies in the lack of common field of view between the EUV imager and the coronagraph.

The real breakthrough on this topic came after the launch of the *Solar Dynamics Observatory* (*SDO*) satellite in 2010. The unprecedentedly high cadence (~ 12 seconds) and high spatial resolution of the aboard Atmospheric Imaging Assembly (AIA) telescope unveiled many details of the kinematics of various EUV waves. Compared to previous instruments, the spatiotemporal resolution of the *SDO*/AIA telescopes is improved so much that the new observations revealed too many subtle features that are sometimes difficult to interpret straightforward [Liu *et al.*, 2010]. However, in a surprisingly weak CME/flare event, the long-awaited two types of waves were finally disclosed clearly [Chen and Wu, 2011]. The time-distance plot of the EUV intensity of this event is displayed in panel (a) of Figure 5, where the faster wave has a velocity of 560 km s^{-1} , whereas the slower wave has a velocity of 190 km s^{-1} . The authors argued that the faster wave corresponds to the coronal Moreton wave, therefore, it is of fast mode; the slower one corresponds to the diffuse “EIT wave” as discovered by Thompson *et al.* [1998]. Since then, more and more events were revealed to have a faster wave ahead of a slower wave, which is best visible from time-distance plots [Schrijver *et al.*, 2011; Asai *et al.*, 2012; Cheng *et al.*, 2012; Shen and Liu, 2012; Kumar *et al.*, 2013; Shen *et al.*, 2013]. Some of these results are displayed in panels (b–d) of Figure 5. In particular, Asai *et al.* [2012] caught the rare chance to observe EUV waves and an $\text{H}\alpha$ Moreton wave simultaneously (panel d in Figure 5), and they confirmed that the faster EUV wave is nearly cospatial with the $\text{H}\alpha$ Moreton wave, whereas the slower wave is behind. An even better example is the 2011 February 14 event analyzed by White *et al.* [2013]. Figure 6 illustrates the time-distance plots in the AIA 211 Å and the *ISOON* $\text{H}\alpha$ wavebands. Their result convincingly confirmed that $\text{H}\alpha$ Moreton wave corresponds to a faster EUV wave, which is followed by a slower yet brighter EUV wave. The two-wave paradigm was recently supported by 3-dimensional MHD simulations [Downs *et al.*, 2012]. In January 2014, a group of “EIT wave” colleagues were gathering in Bern for an International Space Science Institute (ISSI) workshop led by D. Long and S. Bloomfield. Most participants agree that there are two (or at least two) types of EUV waves.

6. What caused the confusion?

The nature of “EIT waves” has been debated for ~ 16 years. It is time to comb the complications and think about what factors led to the controversy among the community.

With respect to $\text{H}\alpha$ Moreton waves, the serious problem is the rarity of the events. Even during only 15 months from 1997 March 24 to 1998 June, about 176 EUV waves were detected by *SOHO*/EIT [Thompson and Myers, 2009]. On the contrary, only dozens of $\text{H}\alpha$ Moreton waves have been observed during the past 55 years. Therefore, it is very rare to find simultaneous Moreton wave and EUV wave observations. The reasons for the rarity of Moreton wave events

include: (1) Only when the coronal shock wave is strong enough, its skirt can heavily sweep the chromosphere so as to generate significant downward motions of the dense chromosphere, i.e., perturbations should exist in many CME/flare events, but in most cases they are not strong enough to produce Doppler shifts of the $\text{H}\alpha$ line; (2) Moreton waves were discovered in $\text{H}\alpha$ -0.5 Å [Moreton and Ramsey, 1960], and it was calculated that the passband around $\text{H}\alpha \pm 0.45 \text{ Å}$ is the best suitable for detecting Moreton waves. However, most of the current $\text{H}\alpha$ telescopes are using $\text{H}\alpha$ line center, with only a few exceptions [e.g., UeNo *et al.*, 2004; Fang *et al.*, 2013].

With respect to EUV waves, the serious problem is the observing cadence. In the *SOHO*/EIT era, i.e., from 1996 to 2006, the cadence of the EUV imaging observations was too low (~ 15 min). However, $\text{H}\alpha$ Moreton waves have relatively short lifetimes, which are generally less than 10 min [Wills-Davey *et al.*, 2007]. The 12-min lifetime of the Moreton wave analyzed by Balasubramaniam *et al.* [2007] is exceptionally long. Therefore, none or at most one front of the Moreton wave can be captured by the *SOHO*/EIT telescope. What the *SOHO*/EIT telescope observed was mainly the slower type of EUV waves. In our opinion, most of them are the EUV counterpart of the CME frontal loop, rather than fast-mode waves or shock waves.

In the *STEREO*/EUVI era, i.e., from 2006 to 2010, the observational cadence was increased to 2.5 min. In principle, several fronts of an Moreton wave event at successive times can be captured, in addition to the slower wave. However, it was demonstrated by Chen and Wu [2011] that, at least for the EUV wave event on 2010 July 27, only when the observational cadence is less than ~ 70 seconds can the two EUV waves be clearly distinguished. This is because both waves originate from the source active region, and they are still not far enough from each other during the lifetime of the faster EUV wave. Only occasionally, for example, when the quiet Sun magnetic field is very weak and the fast-mode wave speed is not very large compared to the sound speed, the two EUV waves might be discernable [Grechnev *et al.*, 2011; Downs *et al.*, 2012].

During the current *SDO*/AIA era, i.e., after 2010, it has been demonstrated that two types of EUV waves can be distinguished well. We were anticipating that a converging consensus should be reached soon [Chen and Fang, 2012]. However, the current state of the “EIT wave” research is still confusing. In our understanding, the confusion in the *SDO*/AIA era is due to the terminology, i.e., “EUV waves” or “coronal waves” were used for both wave phenomena indiscriminately. Among case studies, some events correspond to the fast-mode MHD waves or shock waves [e.g., Li *et al.*, 2012; Yang *et al.*, 2013], whereas some others correspond to the diffusive “EIT waves” [e.g., Zheng *et al.*, 2012b]. Similarly, among statistical studies, some samples mostly consist of the fast-mode MHD waves or shock waves, probably mixed with a few slower wave events. For example, Nitta *et al.* [2013] focused on the fastest wave pattern in the time-distance plot of each event observed by *SDO*/AIA, which they call large-scale coronal propagating fronts (LCPFs). That is why the mean velocity of their LCPFs is as high as 644 km s^{-1} . However, the EUV waves in some other studies mainly belong to the slower type of “EUV waves”, e.g., Muhr *et al.* [2014] investigated the EUV wave kinematics using the *STEREO*/EUVI data and found that the arithmetic mean of the linear velocity is only $254 \pm 74 \text{ km s}^{-1}$. Some colleagues might think that the statistical results of Muhr *et al.* [2014] and Nitta *et al.* [2013] are contradictory. In our personal view, the apparent discrepancy immediately disappears if we consider the waves in Muhr *et al.* [2014] as the slower component and the LCPFs in Nitta *et al.* [2013] as the faster component of the two-wave paradigm. In this sense, the waves called “coronal propagating fronts” by Schrijver *et al.* [2011] belong to the slower

component, very different from the LCPFs in *Nitta et al.* [2013]. Note that, in our viewpoint, a few events in *Nitta et al.* [2013], those with small velocities, should be categorized into the slower component in the two-wave paradigm, where the faster component in these events was too weak to be detected. At the same time, a few events in *Muhr et al.* [2014] might be fast-mode waves. It should be noted here that other two factors may also contribute to the velocity discrepancy between *Nitta et al.* [2013] and *Muhr et al.* [2014]: (1) The cadence of *STEREO/EUVI* is much lower, which would underestimate the propagation velocity [*Long et al.*, 2008]; (2) *Muhr et al.*'s sample was obtained across the solar minimum when the coronal magnetic field is relatively weaker, whereas *Nitta et al.*'s sample was across the solar maximum when the magnetic field is stronger.

From these examples, the readers can see how divergent the current terminologies are. *Chen and Fang* [2012] proposed to use “EIT waves” for the slower component, and “coronal Moreton waves” for the faster component in the two-wave paradigm. Alternatively, we might use “type I EUV waves” for the slower component, and “type II EUV waves” for the faster component. Readers are not obliged to accept such terms, but we do think that it is crucial to have different terms for the two types of EUV waves. Otherwise, controversy will remain forever.

If both the faster and the slower waves appear in one eruption event with the high-cadence observations such as from *SDO/AIA*, it is very easy to disentangle them. However, similar to the case of CMEs where the three components often do not show up simultaneously, the two types of EUV waves are not always present in one event. In the case of only one wave being detected, it becomes important while difficult to clarify which type it belongs to. Based on our limited experience, we propose the following rules. (1) If the wave speed is always subsonic, e.g., below 186 km s^{-1} for the corona with a temperature of 1.5 MK, the observed wave must be the slower component. Since the low corona has a small plasma β , we can even claim that if the wave speed is always below $\sim 300 \text{ km s}^{-1}$, it has a high probability to be the slower component. Note that there are local regions in the corona where the magnetic field strength is close to zero, e.g., the regions near magnetic null points, where the fast-mode wave speed approaches the sound speed, i.e., 186 km s^{-1} . But this happens locally. In most volume of the low corona, the plasma β is much less than unity, otherwise the widely accepted force-free assumption in the coronal magnetic extrapolations [*Low*, 2015] is not valid at all; (2) If the wave speed is above $\sim 500 \text{ km s}^{-1}$, generally the observed wave should be the faster MHD wave or shock wave, i.e., the faster component in the two-wave paradigm; (3) If the wave speed is between the two limits mentioned above, say, $300\text{--}500 \text{ km s}^{-1}$, a range where the two types of EUV waves overlap in velocity, the situation becomes subtle. It depends on other kinematic characteristics, e.g., (i) the slower type of EUV waves would stop near magnetic separatrices [*Delannée and Aulanier*, 1999; *Chen et al.*, 2006; *Chen and Wu*, 2011; *White et al.*, 2013]; (ii) The brightest part of the slower type of EUV waves would rotate anti-clockwise/clockwise in the active region with negative/positive helicity [*Attrill et al.*, 2007]; (iii) The faster type of EUV waves might become concave outward on the solar disk during propagation, resulting from wave refraction [*Xue et al.*, 2013].

7. What are the drivers of the two types of EUV waves?

When Moreton waves were discovered in 1960s [*Moreton and Ramsey*, 1960], people knew nothing about CMEs since the phenomenon was discovered in 1970s [*Tousey*, 1973].

Therefore, solar flares were then ascribed to be the cause of Moreton waves [*Ramsey and Smith*, 1966]. For the same reason, in *Uchida*'s model, Moreton waves were thought to be blast waves generated by the pressure pulse in solar flares [*Uchida*, 1968]. Therefore, Moreton waves were frequently called flare waves [*Zirin and Werner*, 1967; *Vršnak et al.*, 2002]. However, whereas some Moreton waves are accompanied by C-class flares [e.g., *Zhang et al.*, 2011], it is easy to find X-class flares not associated with Moreton waves, e.g., the 2005 January 14 flare studied by *Chen* [2006]. In this case, no CME is accompanied. Therefore, after CMEs were widely studied, it was realized that Moreton waves should be related to CMEs [*Cliver et al.*, 1999; *Chen et al.*, 2002]. Strictly speaking, it is the erupting flux rope that generates the coronal counterpart of an Moreton wave, i.e., a piston-driven shock wave, which straddles over the frontal loop of the CME.

Probably influenced by the early explanation for Moreton waves, after “EIT waves” were discovered, it was initially thought that they might be generated by the pressure pulse of the associated solar flare [e.g., *Warmuth et al.*, 2005], although it was already argued that CME as the driver cannot be ruled out immediately after “EIT waves” were discovered [*Thompson et al.*, 1999; *Wang*, 2000]. In particular, *Delannée* [2000] suggested that “EIT waves” are more related to the magnetic field evolution during CMEs rather than being driven by solar flares. One important reason is that more than half “EIT waves” were associated with tiny flares, such as A- or B-class flares [*Cliver et al.*, 2005]. It is hard to believe that these tiny flares can generate global coronal waves. In order to find out the driver of “EIT waves”, *Chen* [2006] did a test by selecting 14 M- or X-class flares that were not associated with CMEs during solar minima. These flares are ~ 1000 times stronger than the A- or B-class flares in the 1–8 Å soft X-ray flux. If the pressure pulse in A- or B-class flares can generate global coronal waves, there is no reason for M- or X-class flares not to be able to generate global coronal waves. In order to make the test more convincing, *Chen* [2006] chose those flares during solar minima since the relatively quieter corona in the background of the eruption favors the detection of “EIT waves”. *Chen* [2006] found that none of the 14 strong flares was associated with any “EIT wave”. Therefore, they concluded that “EIT waves” are associated with CMEs. Caution should be taken here: people later may occasionally find an “EIT wave” event that is not associated with a visible CME, e.g., the “EIT wave” event studied by *Chen and Wu* [2011]. This is presumably due to the fact that some CMEs are too faint and they are missed by coronagraph observations [*Cheng et al.*, 2005; *Gopalswamy et al.*, 2010; *Wang et al.*, 2011].

Furthermore, after comparing the spatial relationship between an “EIT wave” and the corresponding CME, *Chen* [2009a] found that “EIT waves” are actually cospatial with the CME frontal loop. This was confirmed by *Ma et al.* [2009] and *Dai et al.* [2010]. It means that, when viewed from the side, e.g., for an “EIT wave” happening above the solar limb, it should have a domelike structure as shown by *Chen* [2009a] and *Veronig et al.* [2010]; when an “EIT wave” is observed from the top, e.g., for an “EIT wave” happening on the solar disk, we can see a ringlike front due to projection effects.

In other models mentioned in Section 4, it is also argued that “EIT waves” are strongly related to CMEs. For example, in the successive reconnection model [*Attrill et al.*, 2007], “EIT waves” are formed as the erupting magnetic field reconnects with the neighboring magnetic loops; in the current shell model [*Delannée et al.*, 2008], “EIT waves” are formed at the interface between the erupting core field and the background envelope field.

8. Significance of the research on the two types of EUV waves

We are often confronted with the question: what is the significance to study EUV waves?

First, they are interesting large-scale phenomena in the solar corona, worthy to be understood. Second, EUV waves are strongly correlated with CMEs. Regarding the slower component of the two EUV waves, for example, *Muhr et al.* [2014] found that 95% of the “EIT waves” are associated with CMEs. Considering that some CMEs, especially the halo events, might be missed by coronagraphs [*Cheng et al.*, 2005; *Lara et al.*, 2006; *Gopalswamy et al.*, 2010; *Wang et al.*, 2011], such a result supports the conclusion that there is an unambiguous correlation between EIT waves and CMEs [*Biesecker et al.*, 2002]. Regarding the faster component of the two EUV waves, CMEs are always associated with the LCPFs studied by *Nitta et al.* [2013]. Therefore, either the faster or the slower EUV waves, along with the associated large-scale dimmings, are perfect indicators of CMEs, especially those coming from the front side of the Sun, which have a high chance to hit the Earth. Therefore, in case no coronagraphs are working routinely, EUV imagers can provide reliable information on the possible CMEs from the visible side of the solar disk, which is crucial for space weather forecasting. Third, CMEs are often observed well above the solar limb with coronagraphs occulting the solar disk, the initiation process, which is an extremely important stage in the CME evolution, is often missing in CME observations. Fortunately, it was proposed that the slower component of the EUV waves, i.e., the diffuse “EIT wave”, is actually the EUV counterpart of the CME frontal loop [*Chen*, 2009a]. Therefore, the observations of the diffuse “EIT waves” can fill in the gap, and may provide crucial information for the studies on CME triggering and acceleration. On the other hand, the understanding of the “EIT waves” can shed light on our understanding of the nature of the CME frontal loop. For example, *Chen* [2009a] proposed that in the low corona, say, below a heliocentric distance of $2.5R_{\odot}$, the propagation of the CME frontal loop might be an apparent motion, and its radial velocity in the coronagraph images is not the real plasma velocity. The real plasma velocity might be ~ 3 times smaller than the apparent velocity often registered in all CME catalogs. Fourth, like any other wave phenomenon, EUV waves can also be utilized to diagnose the parameters of the corona, e.g., the magnetic field, which cannot not be measured directly, and some sub-resolution density structures related to the evolution of the amplitude and width of EUV fronts [*Yuan et al.*, 2015]. This is called coronal seismology. Compared to the local seismology in which waves trapped in coronal loops are utilized [*Nakariakov and Verwichte*, 2005], the coronal seismology using EUV waves has the advantage of the large scales since they are observed to cover a major part of the solar disk. However, caution has to be taken when doing the global coronal seismology using EUV waves, since the prerequisite in doing coronal seismology is that we have to be sure what mode the wave is. Whereas there is no objection on the fast-mode wave nature for the faster type of EUV waves, colleagues still have different opinions on the nature of the slower type of EUV waves. When one uses the faster type of EUV waves, with the assumption of a weak fast-mode shock wave, one can derive the reasonable magnetic field strength in the solar corona as done by *Uchida* [1968]. For example, *Long et al.* [2013] applied this type of coronal seismology to a fast-moving ($v = 658 \text{ km s}^{-1}$) EUV wave and obtained the quiet coronal magnetic field strength in the range 2–6 G. Note that they used the term “EIT wave” for the wave phenomenon studied in their paper, but we personally tend to think that it is a faster type of EUV wave. If one applies the same fast-mode wave assumption to the slower diffuse “EIT waves”, one may greatly underestimate the coronal magnetic field. These might include *Ballai and Douglas* [2008] and *West et al.* [2011] among others.

Doing coronal seismology with the slower diffuse “EIT waves” is not impossible, but it is really a formidable task, never so straightforward as the faster type of EUV waves. It

strongly depends on our understanding of the nature of this wavelike apparent phenomenon. So far, several models have been proposed to explain the slower type of EUV waves. It is an interesting issue how these models can be utilized in coronal seismology. One effort was tried by *Chen et al.* [2005b] in the framework of the magnetic fieldline stretching model. Even for the magnetic fieldline stretching model, the inversion from the observed “EIT wave” velocity to the magnetic field strength is extremely difficult. Considering the difficulty of such inversion, *Chen* [2009b] performed a forward modeling, and derive the velocity profile for the slower type of EUV wave for a given 2-dimensional magnetic distribution. In principle, we might adjust the coronal magnetic field in order to make the derived velocity of the slower type of EUV wave best match the observation, and then consider the corresponding 3-dimensional magnetic field to represent the real corona.

9. Summary

To summarize, here we list some important points of this review paper:

(1) As a CME erupts, at least two types of wavelike phenomena might be discernable in EUV images. One is the piston-driven shock wave with a velocity in the range of several hundred to more than 1000 km s^{-1} , the other is not an MHD wave, and the speed is generally below 500 km s^{-1} , sometimes even down to $\sim 10 \text{ km s}^{-1}$.

(2) Whereas the faster EUV is well believed to be a fast-mode MHD shock wave, the nature of the slower wave is still controversial. Even if people agree that the slower EUV wave is actually the CME frontal loop, the formation of the CME frontal loop is still a question to be addressed. We tend to believe that the slower EUV wave is an apparent motion, due mainly to successive magnetic fieldline stretching, and sometimes to magnetic reconnection.

(3) We feel that the current situation is confusing, and the confusion results from the casual usage of the terminologies for EUV waves. We propose that in order to avoid further confusion we need two different names for the two types of EUV waves. One simple option is that they are classified as slow EUV waves and fast EUV waves. The second option is that the slower EUV waves can be called “type I EUV waves” and the faster EUV waves be called “type II EUV waves” since the slower EUV waves should be related to type I radio bursts (both of them result from magnetic field reconfiguration) and the faster EUV waves should be related to type II radio bursts (both of them are from the CME-driven shock, although one may appear without the other, *Nitta et al.* 2014). The third option is that the slower EUV waves can be called “coronal propagating fronts” and the faster EUV waves can be called fast-mode EUV wave/shock wave.

Acknowledgments. The author thanks the organizers for the invitation and two anonymous referees for their thoughtful comments. This research was supported by the grants NSFC (11533005, 11025314, and 10933003) and Jiangsu 333 Project.

References

- Asai, A., et al. (2012), *Astrophys. J.*, , 745, L18, doi: 10.1088/2041-8205/745/2/L18.
- Aschwanden, M. J., et al. (1999), *Astrophys. J.*, , 520, 880–894, doi:10.1086/307502.
- Attrill, G. D. R., et al. (2007), *Astronomische Nachrichten*, 328, 760, doi:10.1002/asna.200710794.
- Attrill, G. D. R., et al. (2014), *Astrophys. J.*, , 796, 55, doi: 10.1088/0004-637X/796/1/55.

- Balasubramaniam, K. S., et al. (2007), *Astrophys. J.*, , 658, 1372–1379, doi:10.1086/512001.
- Ballai, I., and M. Douglas (2008), in *IAU Symposium, IAU Symposium*, vol. 247, edited by R. Erdélyi and C. A. Mendoza-Briceno, pp. 243–250, doi:10.1017/S1743921308014932.
- Banerjee, D., and S. Krishna Prasad (2015), *This volume*, A04104.
- Biesecker, D. A., et al. (2002), *Astrophys. J.*, , 569, 1009–1015, doi:10.1086/339402.
- Carmichael, H. (1964), *NASA Special Publication*, 50, 451.
- Chen, F., et al. (2010), *Astrophys. J.*, , 720, 1254–1261, doi:10.1088/0004-637X/720/2/1254.
- Chen, F., et al. (2011), *Astrophys. J.*, , 740, 116, doi:10.1088/0004-637X/740/2/116.
- Chen, P. F. (2006), *Astrophys. J.*, , 641, L153–L156, doi:10.1086/503868.
- Chen, P. F. (2009a), *Astrophys. J.*, , 698, L112–L115, doi:10.1088/0004-637X/698/2/L112.
- Chen, P. F. (2009b), *Science in China: Physics, Mechanics and Astronomy*, 52, 1785–1789, doi:10.1007/s11433-009-0240-9.
- Chen, P. F. (2011), *Living Reviews in Solar Physics*, 8, 1, doi:10.12942/lrsp-2011-1.
- Chen, P. F., and C. Fang (2012), in *EAS Publications Series, EAS Publications Series*, vol. 55, edited by M. Faurobert, C. Fang, and T. Corbard, pp. 313–320, doi:10.1051/eas/1255043.
- Chen, P. F., and K. Shibata (2002), in *8th Asian-Pacific Regional Meeting, Volume II*, edited by S. Ikeuchi, J. Hearnshaw, and T. Hanawa, pp. 421–422.
- Chen, P. F., and Y. Wu (2011), *Astrophys. J.*, , 732, L20, doi:10.1088/2041-8205/732/2/L20.
- Chen, P. F., et al. (2002), *Astrophys. J.*, , 572, L99–L102, doi:10.1086/341486.
- Chen, P. F., et al. (2005a), *Space Sci. Rev.*, 121, 201–211, doi:10.1007/s11214-006-3911-0.
- Chen, P. F., et al. (2005b), *Astrophys. J.*, , 622, 1202–1210, doi:10.1086/428084.
- Chen, P. F., et al. (2006), *Advances in Space Research*, 38, 456–460, doi:10.1016/j.asr.2005.01.049.
- Cheng, J. X., et al. (2005), in *Coronal and Stellar Mass Ejections, IAU Symposium*, vol. 226, edited by K. Dere, J. Wang, and Y. Yan, pp. 112–113, doi:10.1017/S1743921305000244.
- Cheng, X., et al. (2012), *Astrophys. J.*, , 745, L5, doi:10.1088/2041-8205/745/1/L5.
- Cliver, E. W., et al. (1999), *Solar Phys.*, 187, 89–114, doi:10.1023/A:1005115119661.
- Cliver, E. W., et al. (2005), *Astrophys. J.*, , 631, 604–611, doi:10.1086/432250.
- Cohen, O., et al. (2009), *Astrophys. J.*, , 705, 587, doi:10.1088/0004-637X/705/1/587.
- Dai, Y., et al. (2010), *Astrophys. J.*, , 708, 913–919, doi:10.1088/0004-637X/708/2/913.
- Delaboudinière, J.-P., et al. (1995), *Solar Phys.*, 162, 291–312, doi:10.1007/BF00733432.
- Delannée, C. (2000), *Astrophys. J.*, , 545, 512–523, doi:10.1086/317777.
- Delannée, C., and G. Aulanier (1999), *Solar Phys.*, 190, 107–129, doi:10.1023/A:1005249416605.
- Delannée, C., et al. (2008), *Solar Phys.*, 247, 123–150, doi:10.1007/s11207-007-9085-4.
- Downs, C., et al. (2012), *Astrophys. J.*, , 750, 134, doi:10.1088/0004-637X/750/2/134.
- Eto, S., et al. (2002), *PASJ*, 54, 481–491, doi:10.1093/pasj/54.3.481.
- Fang, C., et al. (2013), *Research in Astronomy and Astrophysics*, 13, 1509, doi:10.1088/1674-4527/13/12/011.
- Forbes, T. G. (2000), *J. Geophys. Res.*, , 105, 23,153–23,166, doi:10.1029/2000JA000005.
- Francile, C., et al. (2013), *Astron. Astrophys.*, , 552, A3, doi:10.1051/0004-6361/201118001.
- Gallagher, P. T., and D. M. Long (2011), *Space Sci. Rev.*, 158, 365–396, doi:10.1007/s11214-010-9710-7.
- Gilbert, H. R., et al. (2008), *The Astrophysical Journal*, 685(1), 629.
- Gopalswamy, N., et al. (2009), *Astrophys. J.*, , 691, L123–L127, doi:10.1088/0004-637X/691/2/L123.
- Gopalswamy, N., et al. (2010), *Twelfth International Solar Wind Conference, 1216*, 452–458, doi:10.1063/1.3395902.
- Grechnev, V. V., et al. (2011), *Solar Phys.*, 273, 461–477, doi:10.1007/s11207-011-9781-y.
- Harra, L. K., and A. C. Sterling (2003), *Astrophys. J.*, , 587, 429–438, doi:10.1086/368079.
- Hudson, H. (1999), *Solar Phys.*, 190, 91–106, doi:10.1023/A:1005246501003.
- Klassen, A., et al. (2000), *A&A Suppl.*, 141, 357–369, doi:10.1051/aas:2000125.
- Krucker, S., et al. (1999), *Astrophys. J.*, , 519, 864–875, doi:10.1086/307415.
- Kumar, P., et al. (2013), *Solar Phys.*, 282, 523–541, doi:10.1007/s11207-012-0158-7.
- Kwon, R.-Y., et al. (2013), *Astrophys. J.*, , 766, 55, doi:10.1088/0004-637X/766/1/55.
- Lara, A., et al. (2006), *Journal of Geophysical Research (Space Physics)*, 111, A06107, doi:10.1029/2005JA011431.
- Li, T., et al. (2012), *Astrophys. J.*, , 746, 13, doi:10.1088/0004-637X/746/1/13.
- Liu, W., and L. Ofman (2014), *Solar Phys.*, 289, 3233–3277, doi:10.1007/s11207-014-0528-4.
- Liu, W., et al. (2010), *Astrophys. J.*, , 723, L53–L59, doi:10.1088/2041-8205/723/1/L53.
- Liu, W., et al. (2012), *Astrophys. J.*, , 753, 52, doi:10.1088/0004-637X/753/1/52.
- Long, D. M., et al. (2008), *Astrophys. J.*, , 680, L81–L84, doi:10.1086/589742.
- Long, D. M., et al. (2013), *Solar Phys.*, 288, 567–583, doi:10.1007/s11207-013-0331-7.
- Low, B. C. (2015), *Science China Physics, Mechanics, and Astronomy*, 58, 2, doi:10.1007/s11433-014-5626-7.
- Ma, S., et al. (2009), *Astrophys. J.*, , 707, 503–509, doi:10.1088/0004-637X/707/1/503.
- Meyer, F. (1968), in *Structure and Development of Solar Active Regions, IAU Symposium*, vol. 35, edited by K. O. Kiepenheuer, p. 485.
- Moreton, G. E., and H. E. Ramsey (1960), *Publ. A. S. P.*, , 72, 357, doi:10.1086/127549.
- Moses, D., et al. (1997), *Solar Phys.*, 175, 571–599, doi:10.1023/A:1004902913117.
- Muhr, N., et al. (2014), *Solar Phys.*, 289, 4563–4588, doi:10.1007/s11207-014-0594-7.
- Nakariakov, V. M., and E. Verwichte (2005), *Living Reviews in Solar Physics*, 2, 3, doi:10.12942/lrsp-2005-3.
- Nakariakov, V. M., et al. (1999), *Science*, 285, 862–864, doi:10.1126/science.285.5429.862.
- Nitta, N. V., et al. (2013), *Astrophys. J.*, , 776, 58, doi:10.1088/0004-637X/776/1/58.
- Nitta, N. V., et al. (2014), *Solar Phys.*, 289, 4589–4606, doi:10.1007/s11207-014-0602-y.
- Ofman, L., and B. J. Thompson (2002), *Astrophys. J.*, , 574, 440–452, doi:10.1086/340924.
- Patsourakos, S., and A. Vourlidas (2009), *Astrophys. J.*, , 700, L182–L186, doi:10.1088/0004-637X/700/2/L182.
- Patsourakos, S., and A. Vourlidas (2012), *Solar Phys.*, 281, 187–222, doi:10.1007/s11207-012-9988-6.
- Patsourakos, S., et al. (2009), *Solar Phys.*, 259, 49–71, doi:10.1007/s11207-009-9386-x.
- Patsourakos, S., et al. (2010), *Astrophys. J.*, , 724, L188–L193, doi:10.1088/2041-8205/724/2/L188.
- Podladchikova, O., and D. Berghmans (2005), *Solar Phys.*, 228, 265–284, doi:10.1007/s11207-005-5373-z.
- Pohjolainen, S., et al. (2001), *Astrophys. J.*, , 556, 421–431, doi:10.1086/321577.
- Ramsey, H. E., and S. F. Smith (1966), *Astron. J.*, , 71, 197, doi:10.1086/109903.
- Schrijver, C. J., et al. (2011), *Astrophys. J.*, , 738, 167, doi:10.1088/0004-637X/738/2/167.
- Selwa, M., et al. (2013), *Solar Phys.*, 284, 515–539, doi:10.1007/s11207-013-0302-z.
- Shen, Y., and Y. Liu (2012), *Astrophys. J.*, , 752, L23, doi:10.1088/2041-8205/752/2/L23.
- Shen, Y., et al. (2013), *Astrophys. J.*, , 773, L33, doi:10.1088/2041-8205/773/2/L33.
- Sterling, A. C., and H. S. Hudson (1997), *Astrophys. J.*, , 491, L55–L58, doi:10.1086/311043.
- Svestka, Z. (1976), *Solar Flares*, 1 ed., Springer-Verlag, Berlin Heidelberg, an optional note.
- Thompson, B. J., and D. C. Myers (2009), *Astrophys. J. (Supp.)*, , 183, 225–243, doi:10.1088/0067-0049/183/2/225.

- Thompson, B. J., et al. (1998), *Geophys. Res. Lett.*, , 25, 2465–2468, doi:10.1029/98GL50429.
- Thompson, B. J., et al. (1999), *Astrophys. J.*, , 517, L151–L154, doi:10.1086/312030.
- Thompson, B. J., et al. (2000), *Solar Phys.*, 193, 161–180, doi:10.1023/A:1005222123970.
- Torsti, J., et al. (1999), *Astrophys. J.*, , 510, 460–465, doi:10.1086/306581.
- Tousey, R. (1973), in *Space Research Conference*, edited by M. J. Rycroft and S. K. Runcorn, pp. 713–730.
- Tripathi, D., and N.-E. Raouafi (2007), *Astron. Astrophys.*, , 473, 951–957, doi:10.1051/0004-6361:20077255.
- Uchida, Y. (1968), *Solar Phys.*, 4, 30–44, doi:10.1007/BF00146996.
- Uchida, Y. (1974), *Solar Phys.*, 39, 431–449, doi:10.1007/BF00162436.
- UeNo, S., et al. (2004), in *Ground-based Instrumentation for Astronomy, Society of Photo-Optical Instrumentation Engineers (SPIE) Conference Series*, vol. 5492, edited by A. F. M. Moorwood and M. Iye, pp. 958–969, doi:10.1117/12.550304.
- Vernazza, J. E., et al. (1981), *Astrophys. J. (Supp.)*, , 45, 635–725, doi:10.1086/190731.
- Veronig, A. M., et al. (2010), *Astrophys. J.*, , 716, L57–L62, doi:10.1088/2041-8205/716/1/L57.
- Vourlidas, A., et al. (2003), *Astrophys. J.*, , 598, 1392–1402, doi:10.1086/379098.
- Vršnak, B., et al. (2002), *Astron. Astrophys.*, , 394, 299–310, doi:10.1051/0004-6361:20021121.
- Wang, H., et al. (2009), *Astrophys. J.*, , 700, 1716–1731, doi:10.1088/0004-637X/700/2/1716.
- Wang, T. (2015), *This volume*, 116, A04104.
- Wang, Y., et al. (2011), *Journal of Geophysical Research (Space Physics)*, 116, A04104, doi:10.1029/2010JA016101.
- Wang, Y.-M. (2000), *Astrophys. J.*, , 543, L89–L93, doi:10.1086/318178.
- Warmuth, A. (2010), *Advances in Space Research*, 45, 527–536, doi:10.1016/j.asr.2009.08.022.
- Warmuth, A., and G. Mann (2011), *Astron. Astrophys.*, , 532, A151, doi:10.1051/0004-6361/201116685.
- Warmuth, A., et al. (2005), *Astrophys. J.*, , 626, L121–L124, doi:10.1086/431756.
- Webb, D. F. (2000), *Journal of Atmospheric and Solar-Terrestrial Physics*, 62, 1415–1426, doi:10.1016/S1364-6826(00)00075-4.
- West, M. J., et al. (2011), *Astrophys. J.*, , 730, 122, doi:10.1088/0004-637X/730/2/122.
- White, S. M., and B. J. Thompson (2005), *Astrophys. J.*, , 620, L63–L66, doi:10.1086/428428.
- White, S. M., et al. (2013), *Technical report of Air Force Research Laboratory*, 22, 1–22.
- Wild, J. P., et al. (1963), *Ann. Rev. Astron. Astrophys.*, 1, 291, doi:10.1146/annurev.aa.01.090163.001451.
- Wills-Davey, M. J. (2006), *Astrophys. J.*, , 645, 757–765, doi:10.1086/504144.
- Wills-Davey, M. J., and G. D. R. Attrill (2009), *Space Sci. Rev.*, 149, 325–353, doi:10.1007/s11214-009-9612-8.
- Wills-Davey, M. J., and B. J. Thompson (1999), *Solar Phys.*, 190, 467–483, doi:10.1023/A:1005201500675.
- Wills-Davey, M. J., et al. (2007), *Astrophys. J.*, , 664, 556–562, doi:10.1086/519013.
- Wu, S. T., et al. (2001), *J. Geophys. Res.*, , 106, 25,089–25,102, doi:10.1029/2000JA000447.
- Xue, Z. K., et al. (2013), *Astron. Astrophys.*, , 556, A152, doi:10.1051/0004-6361/201220731.
- Yang, H. Q., and P. F. Chen (2010), *Solar Phys.*, 266, 59–69, doi:10.1007/s11207-010-9595-3.
- Yang, L., et al. (2013), *Astrophys. J.*, , 775, 39, doi:10.1088/0004-637X/775/1/39.
- Yuan, D., et al. (2015), *Astrophys. J.*, , 799, 221, doi:10.1088/0004-637X/799/2/221.
- Zhang, Y., et al. (2011), *PASJ*, 63, 685–, doi:10.1093/pasj/63.3.685.
- Zhao, X. H., et al. (2011), *Astrophys. J.*, , 742, 131, doi:10.1088/0004-637X/742/2/131.
- Zheng, R., et al. (2012a), *Astrophys. J.*, , 747, 67, doi:10.1088/0004-637X/747/1/67.
- Zheng, R., et al. (2012b), *Astrophys. J.*, , 753, L29, doi:10.1088/2041-8205/753/2/L29.
- Zhukov, A. N. (2011), *Journal of Atmospheric and Solar-Terrestrial Physics*, 73, 1096–1116, doi:10.1016/j.jastp.2010.11.030.
- Zhukov, A. N., et al. (2009), *Solar Phys.*, 259, 73–85, doi:10.1007/s11207-009-9375-0.
- Zirin, H., and S. Werner (1967), *Solar Phys.*, 1, 66–100, doi:10.1007/BF00150304.

Corresponding author: P. F. Chen (chenpf@nju.edu.cn)

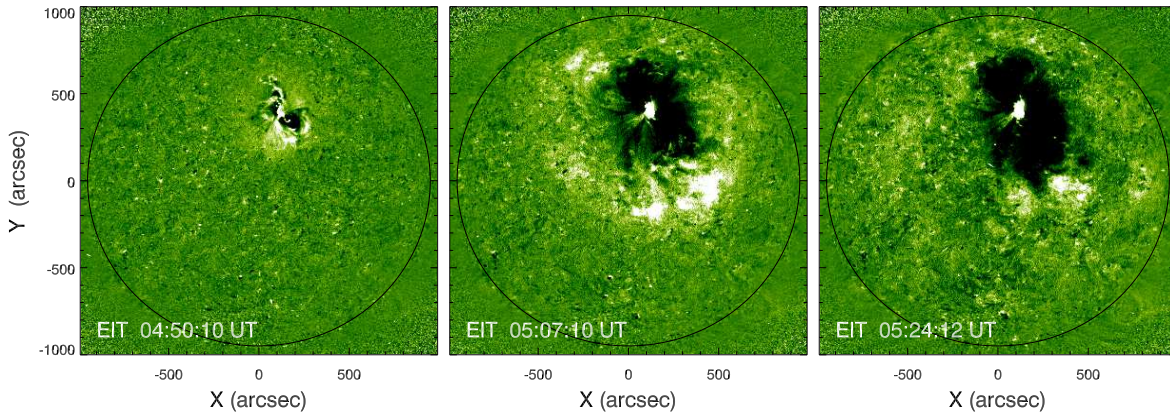


Figure 1. Evolution of the 195 Å based difference intensity map observed by *SOHO*/EIT telescope on 1997 May 12, which was analyzed by *Thompson et al.* [1998], marking the discovery of “EIT waves” [from *Chen*, 2011].

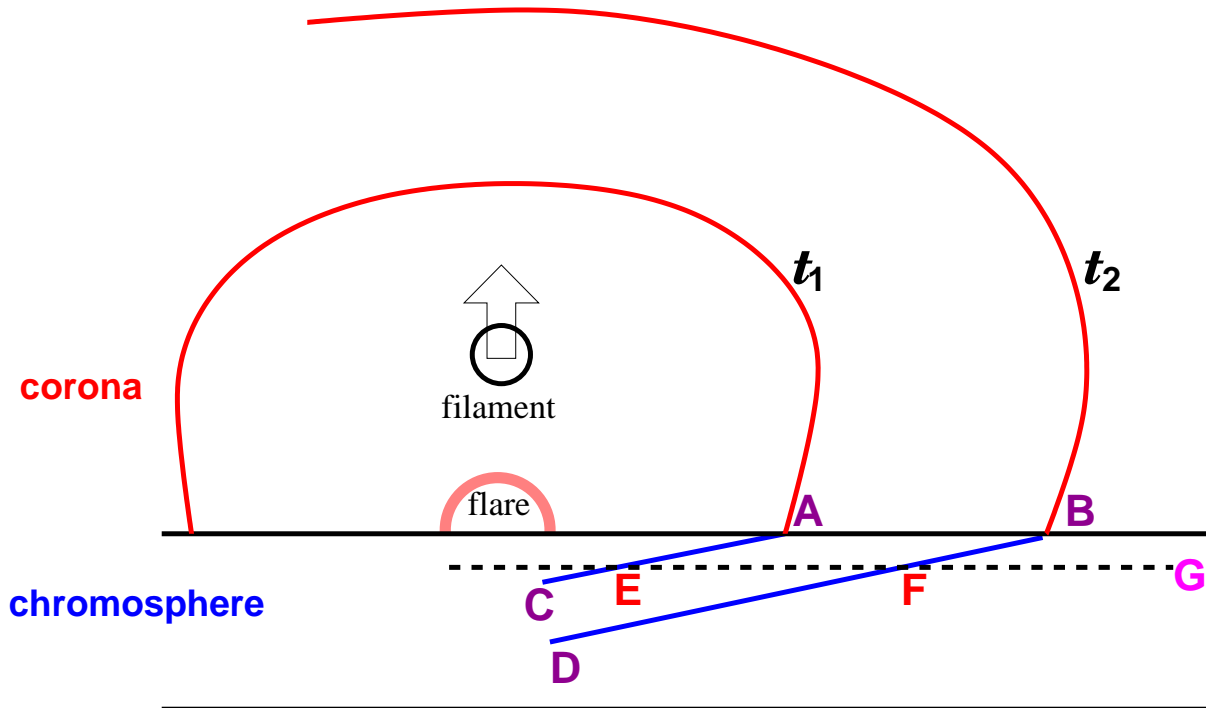


Figure 2. Schematic sketch of Uchida’s model for $H\alpha$ Moreton waves, where the coronal fast-mode MHD wave (or shock wave) sweeps the chromosphere, generating an apparent propagation of the $H\alpha$ Moreton wave from points E to F with the same speed as the coronal fast-mode wave. It is noted that since the amplitude of the fast-mode MHD wave front in the chromosphere decreases drastically as the wave penetrates deeper, not every part of the wave front (*blue lines*) contributes to the observed Moreton wave.

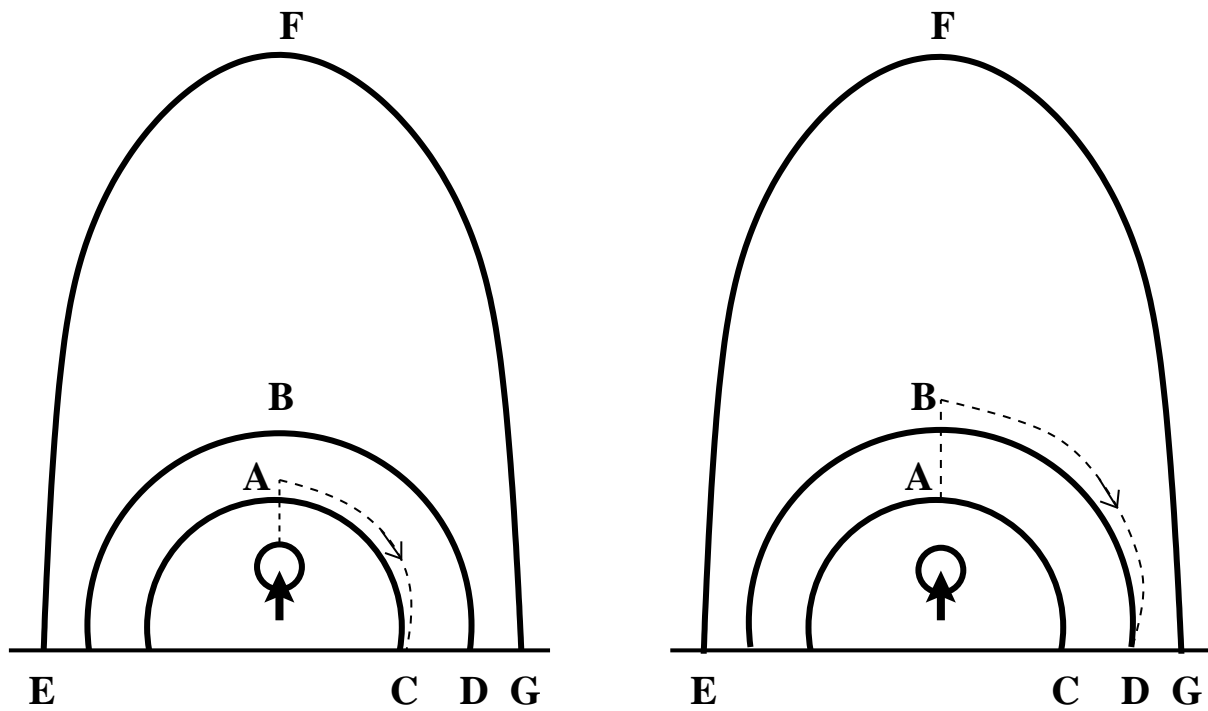


Figure 3. Schematic diagram illustrating how the magnetic fieldline stretching pushed by the erupting flux rope is transferred from the top to the footpoint of each field line so that “EIT wave” fronts are formed successively, from point C to point D at two different times [from *Chen et al.*, 2005b].

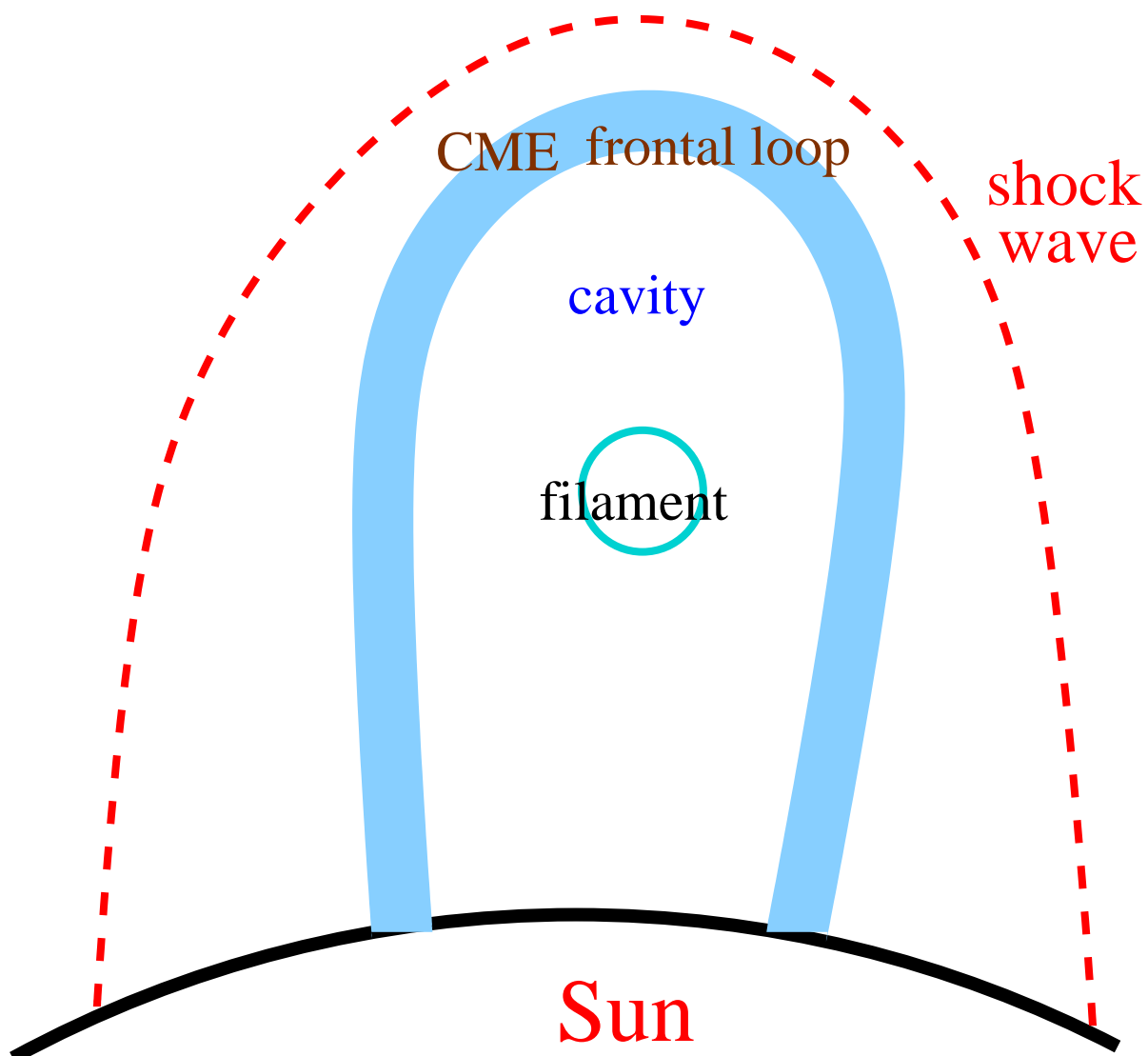


Figure 4. A sketch of the classical 3-component structure (a frontal loop, a bright core representing an erupting filament, and the cavity in between) of a CME observed in white-light.

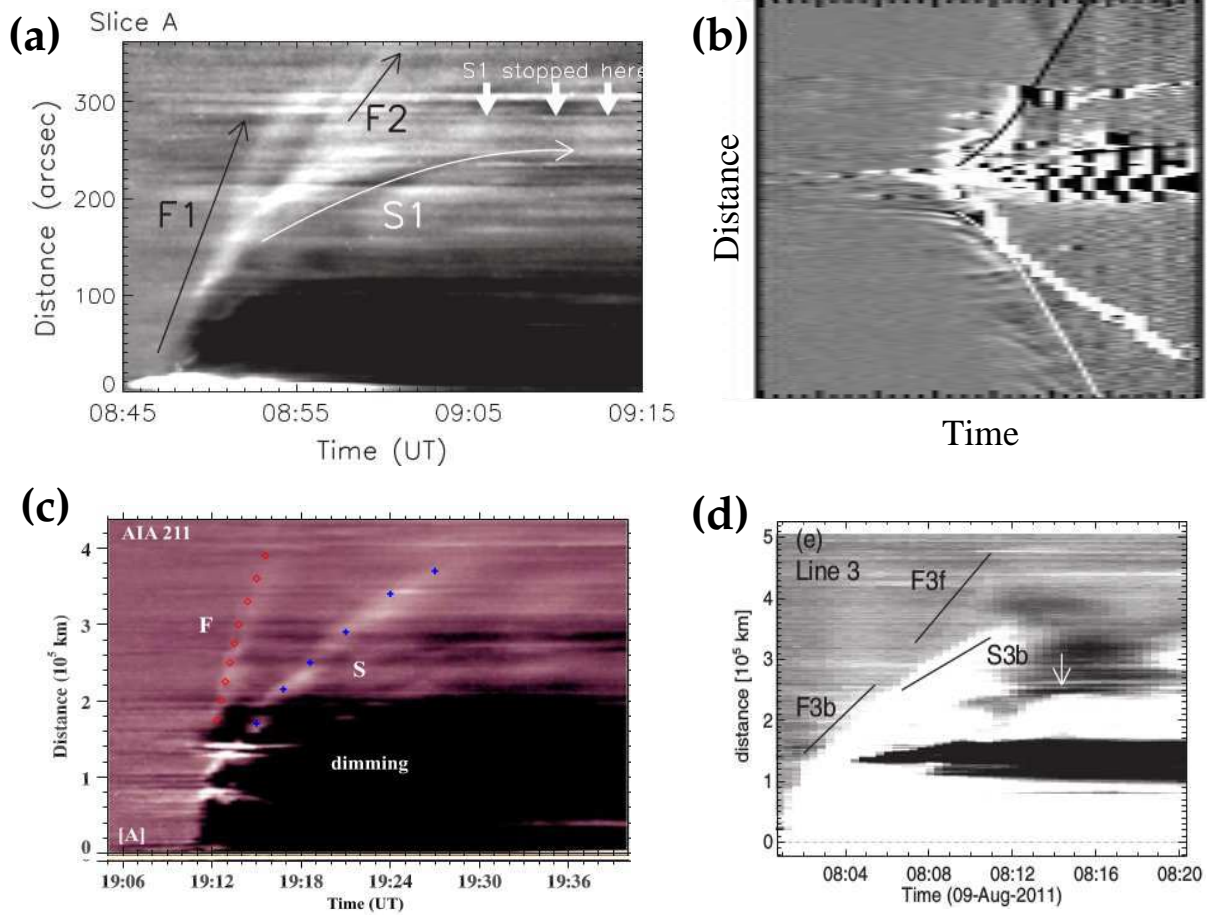


Figure 5. A collection of several time-distance diagrams of the EUV intensity showing two types of EUV waves propagating with different velocities. (a) from *Chen and Wu* [2011]; (b) adapted from *Schrijver et al.* [2011]; (c) adapted from *Kumar et al.* [2013]; and (d) from *Asai et al.* [2012].

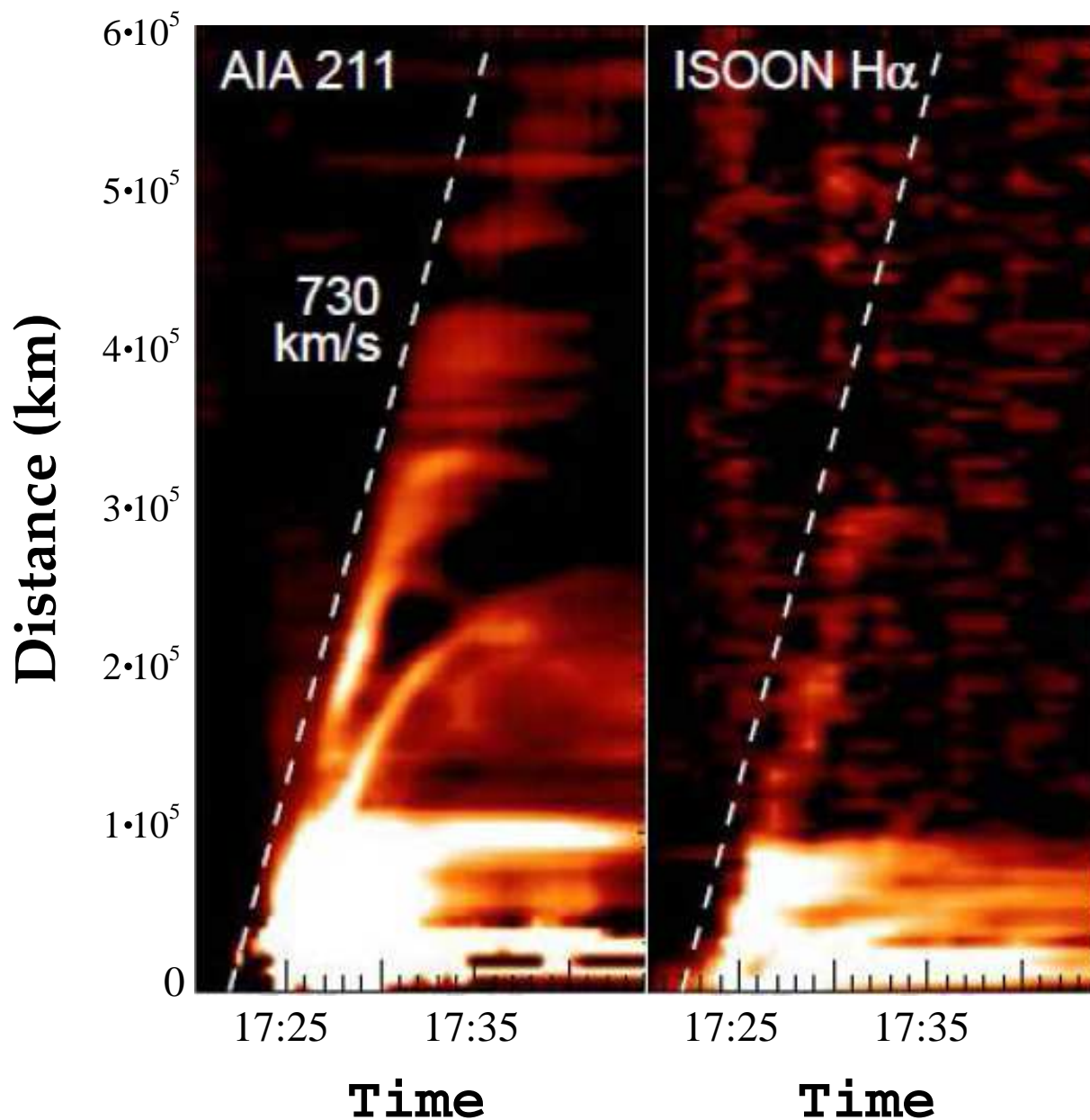


Figure 6. Time-distance diagrams of the AIA 212 Å intensity (*left*) and the *ISOON* H α intensity (*right*), clearly demonstrating the faster EUV wave is nearly cospatial with the H α Moreton wave and the slower EUV wave is much behind [adapted from *White et al.*, 2013].